

Using metal carbonates MCO_3 ($M = Mg^{2+}$, Ca^{2+} , Sr^{2+} and Ba^{2+}) as Auxiliary Compounds to Prepare the YSZ Based Potentiometric CO_2 Sensor

Guangwei Wang^{1,3,*}, Hongzhen Chen^{2,3}, Yuanhui Wu¹

¹ College of Chemistry and Chemical Engineering, Zunyi Normal University, Zunyi, Guizhou, P. R. China, 563006

² MOE Key Laboratory of Groundwater Circulation and Environmental Evolution, China University of Geosciences (Beijing), Beijing, P. R. China, 100083

³ Chongqing Institute of Green and Intelligent Technology (CIGIT), Chinese Academy of Sciences, Chongqing, P. R. China, 400714

*E-mail: wanguangwei@cigit.ac.cn

Received: 26 July 2020 / Accepted: 15 September 2020 / Published: 30 September 2020

Different insoluble carbonates ($MgCO_3$, $CaCO_3$, $SrCO_3$, $BaCO_3$) were introduced into a base material of $Li_2CO_3-Nd_2O_3$, and the formed ternary compounds worked as an auxiliary sensing material in a potentiometric CO_2 sensor. This sensor had YSZ and Au as its solid electrolyte and reference electrode, respectively. By detecting the CO_2 response with each as-prepared sensor before and after a water vapour treatment, the characteristics of the auxiliary sensing compounds were considered. Experimental results indicated that the sensor prepared by the $BaCO_3-Li_2CO_3-Nd_2O_3$ compound exhibited a stable and reproducible response to CO_2 gas over a wide range of 271-576802 ppm. Interestingly, this type of sensor worked well even after a 12-h water vapour treatment at 3 MPa. After further investigations, this sensor may potentially be applied for the practical in situ detection of the CO_2 concentration in a combustion exhaust gas atmosphere.

Keywords: $BaCO_3-Li_2CO_3-Nd_2O_3$; auxiliary sensing compound; YSZ; CO_2 ; sensor

1. INTRODUCTION

The greenhouse effect and other atmospheric issues caused by the increasing emission of CO_2 are causing scientists to be increasingly concerned with the rapid development of industry. As a result, various technologies aimed at treating or reusing emitted CO_2 have been studied in recent years, such as capturing, landfilling, purifying, mineralizing, and deep-sea treatments, along with being reused for chemical reduction, electrochemical conversion and in fuel cells. [1-3]. For the efficient disposal of CO_2 ,

an in situ measurement of its concentration is necessary. Currently, optical and electrochemical methods are the primary techniques for the in situ detection of CO₂ [4-5]. Among these CO₂ measuring methods, the potentiometric CO₂ sensor has the following benefits: a simple theory, low cost, flexible structure, easy production and maintenance, good chemical and mechanical stability, and recognition as one of the most promising methods for the in situ detection of CO₂ in practical industrial processes [6-8].

A potentiometric CO₂ sensor is actually an electrochemical cell composed of three parts: the solid electrolyte (e.g., YSZ), auxiliary sensing electrode (including the CO₂ sensing material and electron conductor) and reference electrode (e.g., conventional gold electrode). During its operation, CO₂ in the detecting system reacts with the sensing material due to the presence of oxygen and an electron conductor, which is one of the main processes of this electrochemical cell. When this reaction is combined with the conversion of oxygen occurring at the reference electrode, a whole sensor cell is formed. Its electromotive force correlates directly with the concentration of CO₂ in the detection system. In this type of potentiometric sensor, the CO₂-associated reaction that occurs on the sensing electrode side is undoubtedly related to the performance of the sensor [9-10]. According to previous studies, carbonates of alkali metals (e.g., Na₂CO₃, Li₂CO₂) are good sensing materials for CO₂ gas, and they have been extensively applied to prepare sensing electrodes for potentiometric CO₂ sensors. However, due to the reaction of these carbonates with some nontargeted components (such as water vapour) probably coexisting during practical use, the performance of the sensor deteriorates after long-term operation [11-13]. Thus, the introduction of good water-resistant materials into the sensing electrode system to form bi- or multicomponent sensing compounds has been thought to be an efficient way to improve the performance of the sensor [14-19].

In this work, several types of water-resistant carbonates of alkaline-earth metals were introduced into the base material of Li₂CO₃-Nd₂O₃, and the formed ternary compounds worked as the auxiliary sensing material in the potentiometric CO₂ sensor; additionally, the sensor has YSZ and Au as its solid electrolyte and reference electrode, respectively. By detecting the CO₂ response of each as-prepared sensor before and after a water vapour treatment, the characteristics of the auxiliary sensing compounds were considered. Experimental results indicated that the sensor prepared by the BaCO₃-Li₂CO₃-Nd₂O₃ compound exhibited a stable and reproducible response to CO₂ gas over a wide concentration range of 271-576802 ppm. Interestingly, this type of sensor works well even after 12 h of treatment in a water vapour atmosphere with a high pressure of up to 3 MPa. After further investigations, this sensor may potentially be applied for the practical in situ detection of CO₂ concentration in an atmosphere of combustion exhaust gas.

2. EXPERIMENTAL

2.1 Preparation of the sensor

The YSZ electrolytes were prepared by the slip casting method from powders of ZrO₂+8 mol% Y₂O₃ (TOSOH TZ 8Y), which were sintered at 1500 °C; subsequently, the samples were shaped into discs with a diameter of 10 mm and a thickness of 2 mm [20]. The surfaces of the discs were polished with 3000 waterproof alumina abrasive paper and cleaned by successively rinsing with hydrochloric

acid, warm n-pentane, acetone, and demineralized water in an ultrasonic bath [21]. The materials used to prepare the auxiliary sensing compounds were analytical reagents. They were weighed according at a mole ratio of 1:1:1 and then milled in a planetary micro-mill for 2 h using a slurry with acetone. Subsequently, the slurry was painted on the surface of one side of a YSZ disc and then dried at 70 °C. Next, the samples were calcined at 730 °C for 1 h in an atmosphere of pure CO₂. Then, Au paste (Kunming Institute of Precious Metals, China) was painted on both the outside of the prepared auxiliary sensing compound and on the other side of the YSZ disc before being sintered at 650 °C for 2 h in air. The prepared carbon dioxide sensor is schematically presented in Fig. 1.

Table 1. Conditions for the preparation of the auxiliary sensing compounds

		Materials		Temperature (°C)	Time (h)
Sensor 1	Li ₂ CO ₃	Nd ₂ O ₃	MgCO ₃	730	1.0
Sensor 2	Li ₂ CO ₃	Nd ₂ O ₃	CaCO ₃	730	1.0
Sensor 3	Li ₂ CO ₃	Nd ₂ O ₃	SrCO ₃	730	1.0
Sensor 4	Li ₂ CO ₃	Nd ₂ O ₃	BaCO ₃	730	1.0

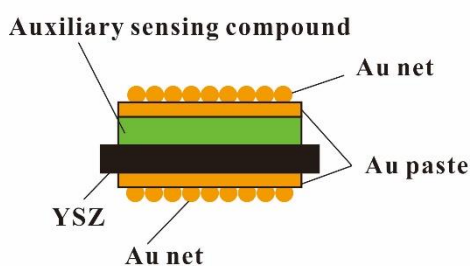


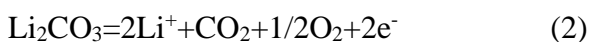
Figure 1. Schematic drawing of the prepared CO₂ sensor

2.2 Electrochemical theory

The prepared YSZ-based potentiometric CO₂ sensor can be written as



At the Au/auxiliary sensing compound interface, the CO₂ and O₂ gases contained in the detecting system react with the carbonates in the auxiliary sensing compound, which is described in equations (2) and (3).



At the Au/YSZ interface, oxygen in the detection system is reduced, as shown in equation (4).



At the auxiliary sensing compound/YSZ interface, Li⁺ and Mg²⁺/Ca²⁺/Sr²⁺/Ba²⁺ react with the oxygen anion that migrates across the YSZ, which is described in equations (5) and (6).



There are 2 theoretical transference electrons in the above equations, and as a result, the electromotive force of the CO₂ sensor can be described by equation (7).

$$EMF = E_0 + \frac{2.303RT}{2F} \lg \left\{ \frac{(P_{O_2})^{1/2} P_{CO_2}}{(P_{O_2})^{1/2}} \right\} \quad (7)$$

Due to the same oxygen partial pressure in the detecting system, equation (7) can be simplified as equation (8).

$$EMF = E_0 + \frac{2.303RT}{2F} \lg(P_{CO_2}) \quad (8)$$

Equation (8) shows the detection mechanism of this type of potentiometric CO₂ sensor. By measuring the electromotive force of the sensor, the content of CO₂ in the system can be determined.

2.3 Detection method

The experimental setup for the CO₂ response detection of the sensor is shown in Fig. 2. In Fig. 2, the test sensor was located at the centre of the reactor, which was fixed in a tube furnace. The sensing electrode and reference electrode of the sensor were pressed together by a Au net and conducted by a Au wire (diameter of 0.2 mm). The Au wires were pulled through Al₂O₃ tubes and then connected with a 34410A voltmeter for the electromotive force measurement. The measuring temperature was 450 °C (±0.5 °C), which was provided by a K-type (NiCr-NiAl) thermocouple placed in proximity of the CO₂ sensor and guided out of the furnace through a two-hole alumina tube. The measuring gas consisted of high purity nitrogen and a CO₂ content gas (balanced by air), all controlled by a high-resolution gas flowmeter (Kyoto 3660). This gas was passed through the reactor at a constant rate of 100 mL/min during the CO₂ response detection test.

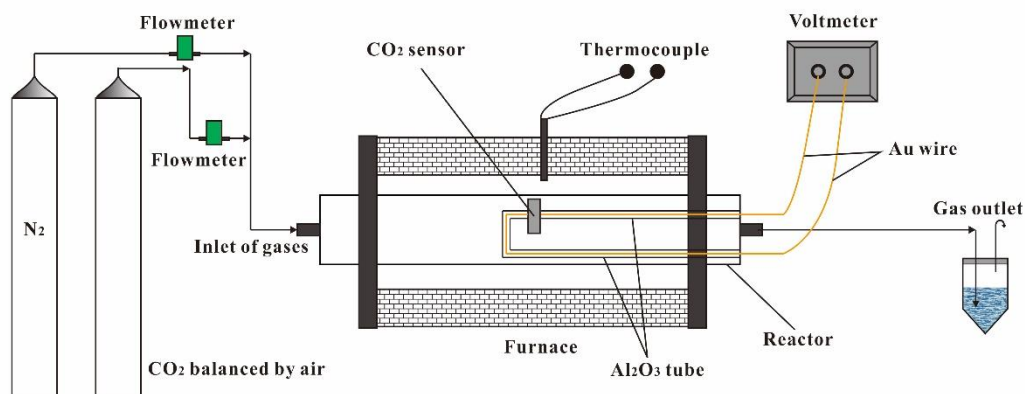


Figure 2. Experimental setup for the CO₂ sensor detection test

3. RESULTS AND DISCUSSION

3.1 Response of the as-prepared sensor

The response of the as-prepared sensor at 450 °C according to changes in CO₂ concentration from 576802 → 271 → 576802 ppm is presented in Fig. 3. As shown in Fig. 3, during the whole process

of changing CO₂, each sensor responds rapidly. As the CO₂ concentration suddenly changes from one point to the next point, the output of the sensor reaches a relatively stable state several minutes later, and subsequently changes very slowly until the next abrupt alteration in CO₂ concentration. The EMF curves exhibit symmetrical characteristics during both the decreasing period (576802 → 271 ppm) and increasing period (271 → 576802 ppm) in the CO₂ concentration. These results indicate that each as-prepared sensor has acceptable EMFs when the concentration of CO₂ in the detecting system remains constant.

According to equation (8), the relationship between the stable EMFs and the corresponding CO₂ concentrations is plotted in Fig. 4. In Fig. 4, each sensor behaves linearly, and the fitting lines seem very close to each other. When the concentration of CO₂ is low, the fitting lines almost overlap. By using the slopes of the fitting lines presented in Fig. 4, the number of transference electrons (n) and the EMF change rate that corresponds to the logarithm of CO₂ concentration for the practical electrochemical process of the sensor (ΔE) can be conveniently obtained, and the results are presented in Table 2. Combined with Fig. 3 and Fig. 4, each as-prepared sensor has a similar number of transference electrons, which is close to the theoretical value of 2 at the experimental temperature and over the range of CO₂ concentrations. All four types of sensors respond rapidly and correctly with the changes in CO₂ concentration, while exhibiting Nernst characteristics.

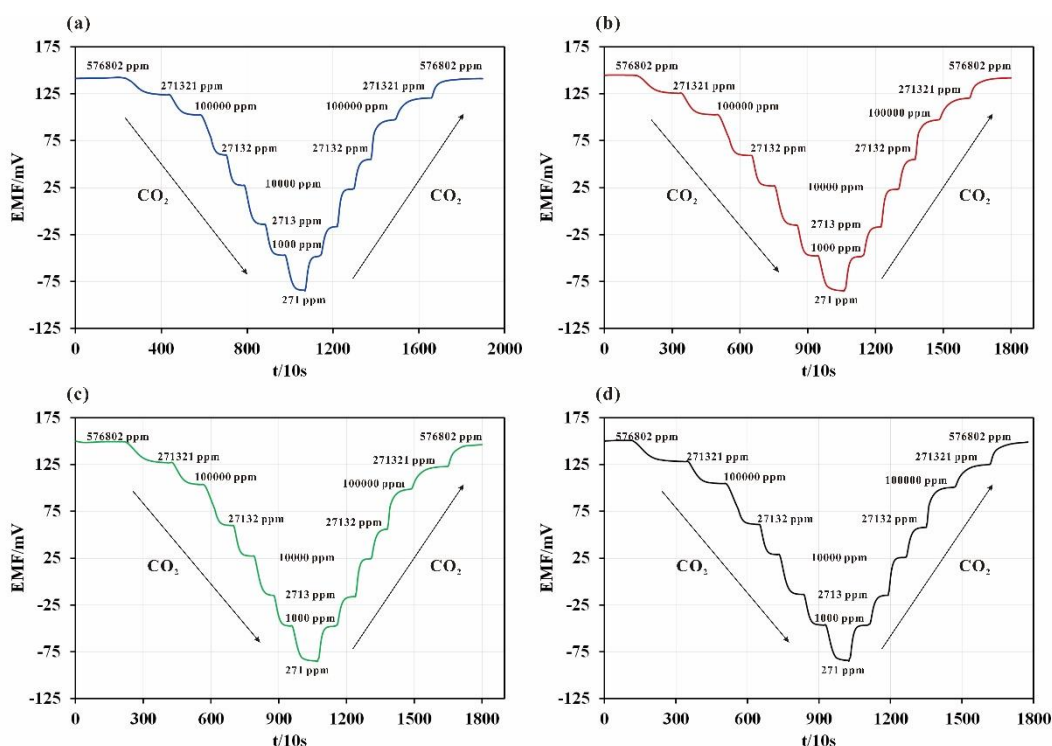


Figure 3. Responses of the as-prepared sensors at 450 °C and with the continuous change in CO₂ concentration from 576802 → 271 → 576802 ppm: (a) Sensor 1, (b) Sensor 2, (c) Sensor 3, and (d) Sensor 4.

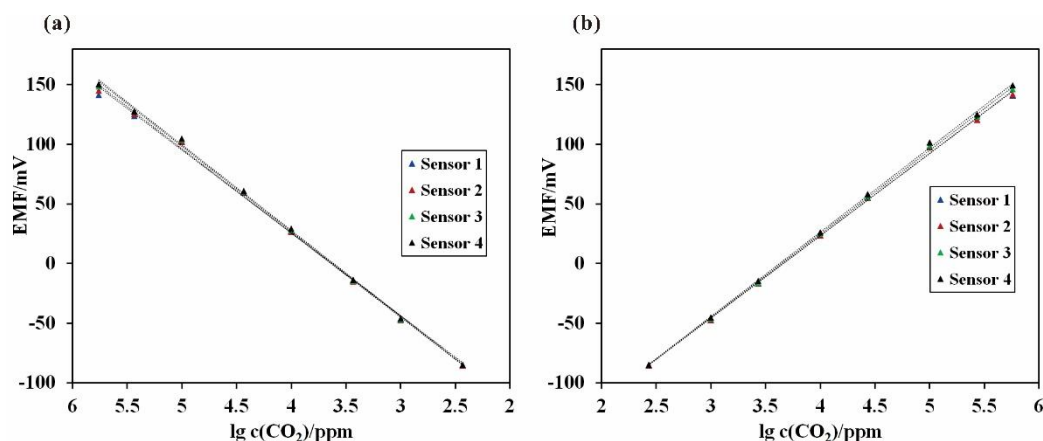


Figure 4. Relationship between the stable EMFs of the as-prepared sensor and the corresponding CO₂ concentrations at 450 °C, and with the continuous change in CO₂ concentration from 576802 →271 →576802 ppm: (a) CO₂ decreased from 576802 to 271 ppm and (b) CO₂ increased from 271 to 576802 ppm.

Table 2. Number of transference electrons (*n*) and the EMF change rate (ΔE) of the as-prepared sensors at 450 °C with a continuous change in CO₂ concentration from 576802 →271 →576802 ppm.

	Sensor 1		Sensor 2		Sensor 3		Sensor 4	
	CO ₂ ↓	CO ₂ ↑						
<i>n</i>	2.06	2.08	2.03	2.07	2.01	2.04	2.00	2.02
ΔE (mV)	69.55	68.84	70.59	69.18	71.42	70.18	71.59	70.79

3.2 Response of the sensor after a water vapour treatment

In this work, insoluble carbonates and Nd₂O₃ were introduced into Li₂CO₃ to form sensing compound materials. To evaluate the water vapour resistance of the auxiliary sensing compounds, each sensor was pretreated at 450 °C for 12 h in an atmosphere consisting of 10% water vapour. The responses of the pretreated sensors are presented in Fig. 5. According to Fig. 5, the EMF outputs of Sensors 1, 2 and 3 for the same amount of CO₂ decrease substantially compared with those without a water vapour treatment (Fig. 3). The decreases in the EMFs with changing CO₂ concentration are more obvious during the decreasing period (576802 →271 ppm) than during the increasing period (271 →576802 ppm). Furthermore, the stability of the sensor output decreases compared with that without a water vapour treatment. Among the four types of sensors, Sensor 4 shows the smallest effect from the water vapour treatment. During the changes in CO₂ concentration, Sensor 4 has symmetrical responses during the decreasing and increasing periods, as shown in Fig. 3. According to the fitting lines shown in Fig. 6, the correlations among the stable EMFs and the corresponding CO₂ concentrations, number of transference electrons (*n*) and EMF change rates (ΔE) are presented in Table 3. Based on the experimental results presented in Fig. 6 and Table 3, Sensor 4 exhibits an acceptable number of transference electrons and EMF change rate when compared with that in Table 2, which demonstrates the good water vapour resistance of this type of sensor. However, Sensors 1, 2 and 3 have transference electron numbers that

deviate from the original values, which are close to 2. Additionally, the EMF change rates decrease substantially due to the water vapour treatment, which will produce a large error in practical applications.

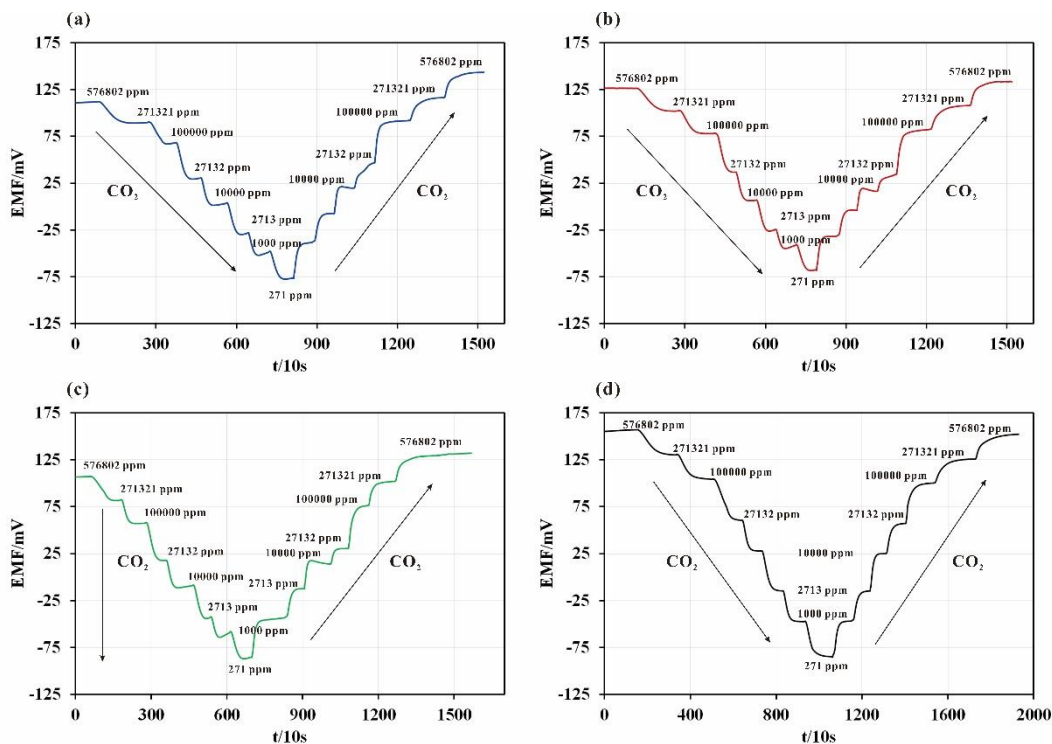


Figure 5. Responses of the sensors after a 12-h pretreatment in a 10% water vapour atmosphere at 450 °C: (a) Sensor 1, (b) Sensor 2, (c) Sensor 3, and (d) Sensor 4.

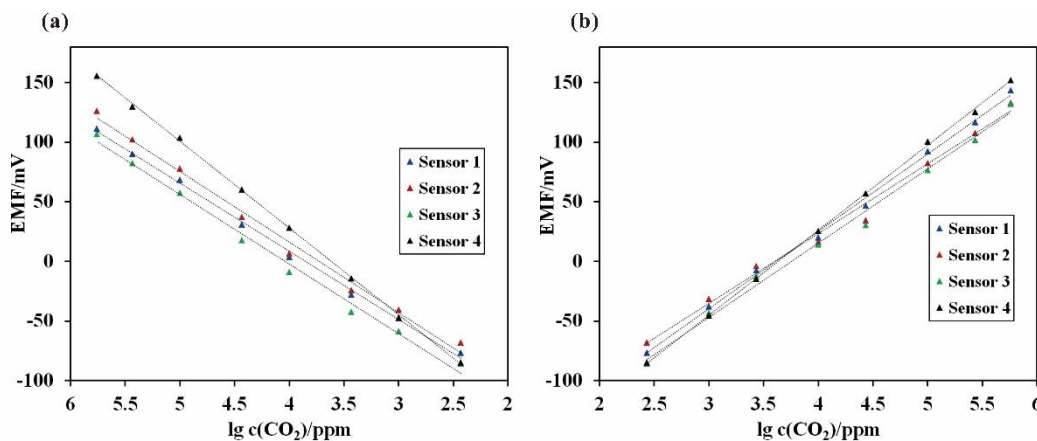


Figure 6. Relationship between the stable EMFs of the sensors after the water vapour treatment and with the continuous change in CO₂ concentration from 576802 → 271 → 576802 ppm at 450 °C: (a) CO₂ decreased from 576802 to 271 ppm and (b) CO₂ increased from 271 to 576802 ppm.

In this work, the percentage of response (POR) of the sensor is defined as the ratio of practical output EMFs with the theoretical output EMFs due to the change in CO₂ concentration from the lowest value of 271 ppm to the highest value of 576802 ppm and vice versa. To compare the performance of each sensor before and after the water vapour treatment, the POR values of the sensors are computed and presented in Fig. 7. In Fig. 7, Sensor 4 has similar POR values before and after the water vapour

treatment, and its POR values are much higher than those of the other sensors. These results indicate that Sensor 4 exhibits acceptable EMFs even after the 12-h water vapour treatment.

Table 3. Number of transference electrons (n) and the EMF change rates (ΔE) of sensors after the water vapour treatment at 450 °C and during the continuous change in CO₂ concentration (576802 →271 →576802 ppm).

	Sensor 1		Sensor 2		Sensor 3		Sensor 4	
	CO ₂ ↓	CO ₂ ↑						
n	2.51	2.21	2.42	2.45	2.46	2.30	1.97	2.01
ΔE (mV)	57.17	65.01	59.24	58.52	58.40	62.29	72.58	71.26

However, the POR values of Sensors 1, 2 and 3 decrease because of the water vapour treatment, which may cause large detection errors during practical applications. Before the water vapour treatment, the four types of sensors have similar POR values during both the decreasing and increasing periods of changing CO₂ concentration. However, only Sensor 4 is hardly affected by the increasing/decreasing changes in CO₂. The other three types of sensors exhibit much smaller response percentages during the decreasing CO₂ concentration compared with that during the increasing CO₂ concentration. In a practical exhaust gas atmosphere, the concentration of CO₂ fluctuates at random. As a result, Sensor 4 has the advantage over the other three types of sensors for practical application in industry. However, the mechanism by which the increasing/decreasing change in CO₂ concentration affects the water vapour-treated sensors is worthy of further investigation.

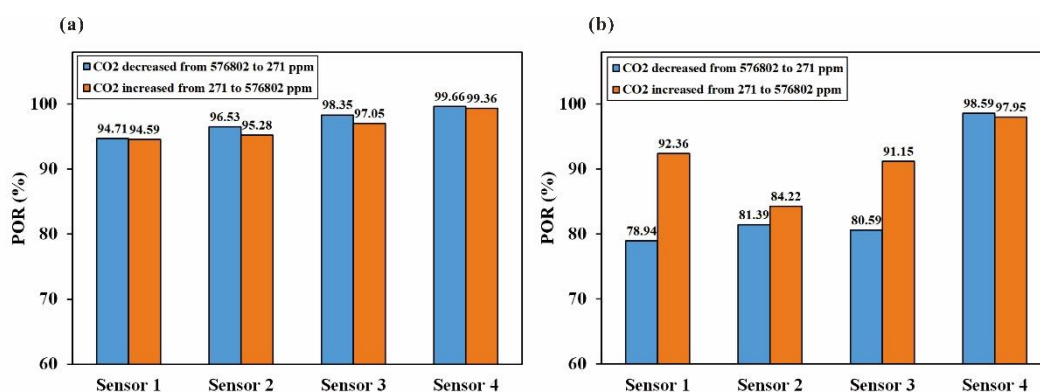


Figure 7. Percentage of response (POR) values of the sensors at 450 °C and with the continuous change in CO₂ concentration from 576802 →271 →576802 ppm: (a) before the water vapour treatment and (b) after the water vapour (10%) treatment.

To further understand the performance of Sensor 4, its response with the opposite change in CO₂ concentration (271 →576802 →271 ppm) was obtained; the results are shown in Fig. 8. In Fig. 8, Sensor 4 exhibits a similar CO₂ response before and after the water vapour treatment. Sensor 4 responds rapidly to the abrupt changes in CO₂ concentration and quickly reaches stable EMFs. Furthermore, Sensor 4 exhibits symmetrical characteristics during increasing CO₂ concentration (271 →576802 ppm) and

decreasing CO₂ concentration (576802 → 271 ppm). Combined with Fig. 3 and Fig. 5, Sensor 4 has acceptable EMFs at the same CO₂ concentrations. The stable EMFs at each point are hardly affected by both the increasing/decreasing change in CO₂ concentration and the water vapour, which indicates the good stability of Sensor 4.

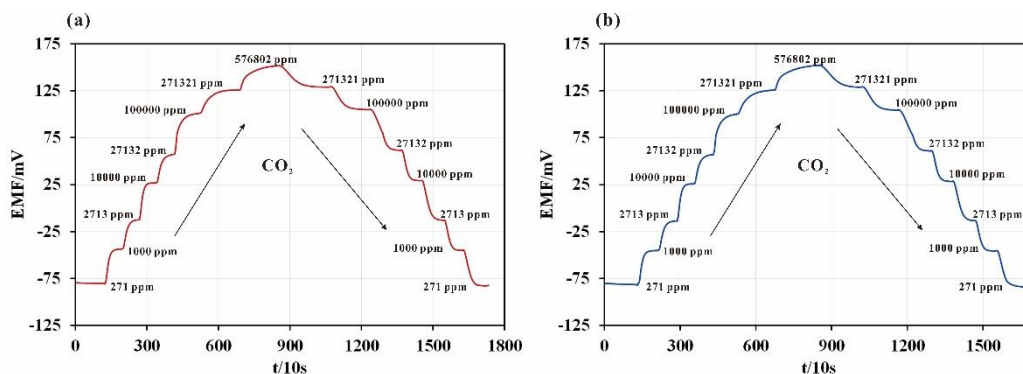


Figure 8. Response of Sensor 4 at 450 °C and with the continuous change in CO₂ concentration from 271 → 576802 → 271 ppm: (a) before the water vapour treatment and (b) after the water vapour (10%) treatment.

According to the experimental results of Sensor 4, which underwent the water vapour treatment for 12 h, the auxiliary sensing compound of Li₂CO₃-Nd₂O₃-BaCO₃ exhibits not only sensing properties for CO₂ gas but also good water vapour resistance. However, in some practical industries, the CO₂ sensor is probably used in an atmosphere at high pressure.

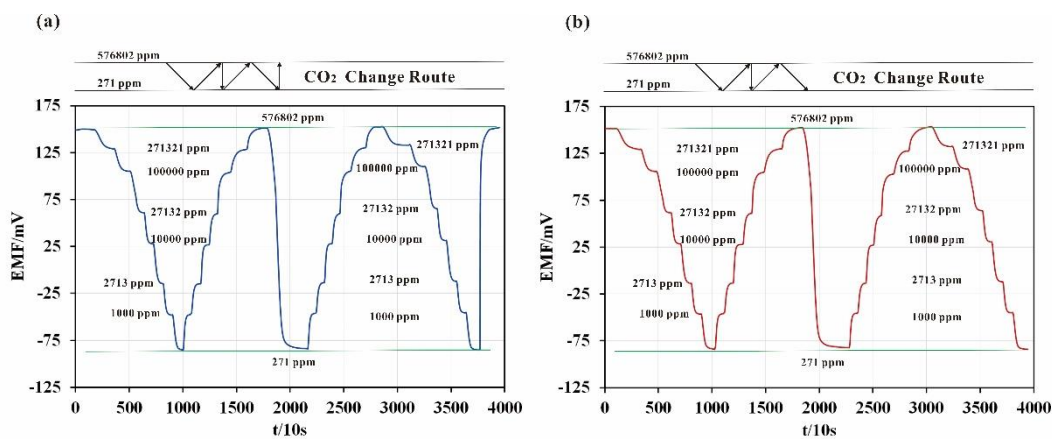


Figure 9. Response of Sensor 4 pretreated in an autoclave with water vapour (10%) at elevated pressures: (a) pretreated at 1 MPa and (b) pretreated at 3 MPa.

To further consider the stability of Sensor 4, it was treated in an autoclave at elevated pressures of 1 and 3 MPa. For each treatment, the time was 12 h, the temperature was controlled at 450 °C, and the atmosphere in the autoclave consisted of nitrogen (90%) and water vapour (10%). After the pretreatment, the responses of the sensors were obtained, and the results are presented in Fig. 9. From

Fig. 9, Sensor 4 exhibits a good response for the continual change in CO₂ concentration, and the sensor that was treated at 1 MPa behaves similarly to the sensor treated at 3 MPa. Both sensors have stable and reproducible responses for the continuous change in CO₂ concentration, although they were treated in an autoclave with water vapour at high pressures. After further improvements, this type of CO₂ sensor may potentially be used to detect the CO₂ concentration in a practical atmosphere of combustion exhaust gas.

To improve the water vapour resistance of the solid potentiometric CO₂ sensor, many studies have been conducted by researchers. M enil studied the Lisicon-based CO₂ sensor and found that the introduction of CaCO₃ or BaCO₃ into the auxiliary sensing material could improve its resistance to water vapour [22]. Lee prepared a CO₂ sensor by using Li₃PO₄ as the solid electrolyte and Li₂CO₃-BaCO₃ as the auxiliary sensing material and found that the sensor was not obviously affected by water vapour over a CO₂ range of 500 -200000 ppm compared with a sensor using pure Li₂CO₃ as its auxiliary sensing material [23]. To improve the performance of the electrochemical CO₂ sensor, the Imanaka group carried out many highly effective works. They prepared a potentiometric CO₂ sensor by applying a multi-valent ionic (e.g., Mg²⁺, Zr⁴⁺) conductor and YSZ as the composite solid electrolyte; furthermore, they used a Li and Ba co-doped oxycarbonate to cover the outside surface of the multi-valent ionic conductor chip as the auxiliary sensing material. This type of sensor worked well over a relatively wide range of O₂ concentrations (5-40%) and exhibited good water vapour resistance and long-term stability [24-25]. Tamura used a type of Al³⁺ conductor ((Al_{0.2}Zr_{0.8})_{20/19}Nb(PO₄)₃) and YSZ as the composite solid electrolyte and a compound formed by 0.5(0.8La₂O₂SO₄-0.2Li₂CO₃) and 0.5(Nd_{0.47}Ba_{0.12}Li_{0.29})₂O_{0.94}CO₃ as the auxiliary sensing electrode. The prepared sensor demonstrated not only a Nernst response for the change in CO₂ at 500  C but also good water vapour resistance and an obviously weakened dependency on the oxygen content [26]. In our previous study, the CO₂ potentiometric sensor had a Li and Ba co-doped oxycarbonate as the auxiliary sensing material, which behaved well in a water vapour atmosphere for a relatively long period of time; additionally, this sensing material behaved well to some extent after a constant water vapour treatment at 300  C [27]. Using the compound of Li₂CO₃-Nd₂O₃ as the auxiliary electrode material, the humidity resistance of the Nasicon based CO₂ sensor was improved obviously [28]. In this work, the compound was formed by sintering a mixture of Nd₂O₃, Li₂CO₃ and BaCO₃ at 730  C and in an atmosphere of CO₂. The product probably contains an insoluble structure of oxycarbonate, and the ionic metals (e.g., Li⁺, Ba²⁺) may combine with carbonate ions to form composite carbonates. These compounds can react with CO₂ during operation, and the extent of this reaction is presented by the electromotive force of the sensor. As a result, the content of CO₂ and its change in the detection system can be measured.

4. CONCLUSIONS

Different insoluble carbonates (MgCO₃, CaCO₃, SrCO₃, BaCO₃) were introduced into the base material of Li₂CO₃-Nd₂O₃, and the formed ternary compounds worked as the auxiliary sensing material in a potentiometric CO₂ sensor. This sensor had YSZ and Au as its solid electrolyte and reference electrode, respectively. By detecting the CO₂ response of each as-prepared sensor before and after a

water vapour treatment, the characteristics of the auxiliary sensing compounds were considered. The experimental results indicated that the sensor prepared by the BaCO₃-Li₂CO₃-Nd₂O₃ compound exhibited a stable and reproducible response to CO₂ gas over a wide range of 271-576802 ppm. Interestingly, this type of sensor worked well even after a 12-h water vapour treatment at 3 MPa. After further investigations, this sensor may potentially be applied for the practical in situ detection of the CO₂ concentration in a combustion exhaust gas atmosphere.

ACKNOWLEDGEMENTS

This work was financially supported by the National Natural Science Foundation of China (No. 41763008), the Natural Science and Technology Foundation of Guizhou Provincial Department of Education (No. [2017]086 and No. [2018]004), the Natural Science and Technology Foundation of Guizhou Province (No. [2019]1461), the Technologies R&D Programme of Guizhou Province (No. [2018]2774), the Doctor Foundation of Zunyi Normal University (Zunshi BS [2017]02), and the Open Funding of MOE Key Laboratory of Groundwater Circulation and Environmental Evolution.

References

1. A. Rafiee, K.R. Khalilpour, D. Milani and M. Panahi, *J. Environ. Chem. Eng.*, 6 (2018) 5771.
2. E. Alper and O.Y. Orhan, *Pet.*, 3 (2017) 109.
3. M. Aresta, A. Dibenedetto and E. Quaranta, *J. Catal.*, 343 (2016) 2.
4. M. Henfling, U. Gossner, C. Kutter, W. Hansch and S. Trupp, *Sens. Actuators, B*, 241 (2017) 1256.
5. C. Schwandt, R.V. Kumar and M.P. Hills, *Sens. Actuators, B*, 265 (2018) 27.
6. N. Miura, Y. Yan, M. Sato, S. Yao, S. Nonaka, Y. Shimizu and N. Yamazoe, *Sens. Actuators, B*, 24-25 (1995) 260.
7. N. Miura, Y. Yan, S. Nonaka and N. Yamazoe, *J. Mater. Chem.*, 5 (1995) 1391.
8. H. Näfe and F. Aldinger, *Sens. Actuators, B*, 69 (2000) 46.
9. J.W. Fergus, *Sens. Actuators, B*, 134 (2008) 1034.
10. M. Morio, T. Hyodo, Y. Shimizu and M. Egashira, *Sens. Actuators, B*, 139 (2009) 563.
11. M. Alonso-Porta and R.V. Kumar, *Sens. Actuators, B*, 71 (2000) 173.
12. Y. Shimamoto, T. Okamoto, H. Aono, L. Montanaro and Y. Sadaoka, *Sens. Actuators, B*, 99 (2004) 141.
13. T. Okamoto, Y. Shimamoto, N. Tsumura, Y. Itagaki, H. Aono and Y. Sadaoka, *Sens. Actuators, B*, 108 (2005) 346.
14. T. Kida, K. Shimanoe, N. Miura and N. Yanazoe, *Sens. Actuators, B*, 75 (2001) 179.
15. P. Pasierb, S. Komornicki, R. Gajerski, S. Koziński and M. Rękas, *Solid State Ionics*, 157 (2003) 357.
16. J.S. Lee, J.H. Lee and S.H. Hong, *Sens. Actuators, B*, 96 (2003) 663.
17. M. Yamauchi, Y. Itagaki, H. Aono and Y. Sadaoka, *J. Eur. Ceram. Soc.*, 28 (2008) 27.
18. C. Belda, M. Fritsch, C. Feller, D. Westphal and G. Jung, *Microelectron. Reliab.*, 49 (2009) 614.
19. L. Satyanarayana, W.S. Noh, W.Y. Lee, G.H. Jin and J.S. Park, *Mater. Chem. Phys.*, 114 (2009) 827.
20. J. Dou, H. Li, L. Xu, L. Zhang and G. Wang, *Rare Met.*, 28 (2009) 372.
21. G. Wang and H. Chen, *Int. J. Electrochem. Sci.*, 15 (2020) 9416.
22. F. Ménil, B. O. Daddah, P. Tardy, H. Debéda and C. Lucat, *Sens. Actuators, B*, 107 (2005) 695.
23. I. Lee, S.A. Akbar and P.K. Dutta, *Sens. Actuators, B*, 142 (2009) 337.
24. N. Imanaka, A. Ogura, M. Kamikawa and G. Adachi, *Electrochem. Commun.*, 3 (2001) 451.

25. N. Imanaka, M. Kamikawa and G. Adachi, *Anal. Chem.*, 74 (2002) 4800.
26. S. Tamura, I. Hasegawa, N. Imanaka, T. Maekawa, T. Tsumiishi, K. Suzuki, H. Ishikawa, A. Ikeshima, Y. Kawabata, N. Sakita and G. Adachi, *Sens. Actuators, B*, 108 (2005) 359.
27. G. Wang, H. Chen, Y. Li, B. Xie and Z. Jiang, *Chin. J. Mater. Res.*, 33 (2019) 713.
28. H. Aono, Y. Itagaki and Y. Sadaoka, *Sens. Actuators, B*, 126 (2007) 406.

© 2020 The Authors. Published by ESG (www.electrochemsci.org). This article is an open access article distributed under the terms and conditions of the Creative Commons Attribution license (<http://creativecommons.org/licenses/by/4.0/>).